AI-based condition monitoring of a variable displacement axial piston pump

Abid Abdul Azeez*, Elina Vuorinen*, Tatiana Minav* and Paolo Casoli**

Tampere University, Innovative Hydraulics and Automation (IHA), Korkeakoulunkatu 6, 33720 Tampere,Finland*
University of Parma, Department of Engineering and Architecture, Parco Area delle Scienze, 181/A 43124Parma, Italy**

E-Mail: abid.azeez@tuni.fi

Conventional condition monitoring involves integration of additional sensors for fault detection and diagnosis. They are costly and sensitive to faults themselves. To overcome these issues and data scarcity, simulation model data is used as a source of training data for Artificial Intelligence based condition monitoring of the axial piston pump. The sensitivity of the simulation model is improved by performing data augmentation. The classification of faults for condition monitoring in the model is performed by developing a classifier utilizing machine learning algorithm. This was tested for experimental, simulation, and augmented simulation data with respective accuracy scores of 84.8%, 70.1%, and 75.7%. Hence, augmented simulation data is a suitable option for online condition monitoring.

Keywords: Axial piston pump, Condition monitoring, Classifier, Spectral Analysis
Target audience: Mobile Hydraulics, Design Process, Condition Monitoring

1 Introduction

Axial piston pumps are widely utilized in industrial and off-road mobile applications, such as forestry, agriculture, and mining. They are one of the main components of the hydraulic system to enable high output flow and efficiency. However, these qualities along with the reliability of a pump can be affected by failures, which can also influence the operation of the machine and, therefore, cause unnecessary downtime due to unplanned maintenance. With higher fault tolerance, condition-based monitoring, and maintenance, these potential failures could be identified before major damage occurs minimizing downtime and unnecessary costs from maintenance [1]. To diagnose failures in hydraulic systems, different approaches have been applied, including model-based [2], and instrumental techniques, such as vibration-signal [3],[4], cyclostationary analysis [5], acceleration signal [6], and temperature sensors [7],[8]. To classify failures, various approaches have been implemented, e.g., extreme learning machine (ELM) [9], extreme-point symmetric mode decomposition and random forests [10], symmetrical polar coordinate image and fuzzy c-means clustering algorithm [11], convolutional neural network (CNN) [12], and multi-layer perceptron (MLP) [13].

Conventionally, the condition monitoring system generally involves integration of additional sensors to the system under study for fault detection and diagnosis. However, such systems are themselves costly and are sensitive to faults. Consequently, the current trend is artificial intelligence (AI)-based condition monitoring. These methods rely on data generated from simulation models for condition monitoring rather than utilizing multi-sensor measurements as in the case of conventional condition monitoring [13]. Hence, a simulation model that is validated using experimental data can be adapted as a source of training data for AI-based condition monitoring.

Thus, consequently, a new approach of utilizing machine learning algorithms and data from simulation model for condition monitoring of a variable displacement axial piston pump is applied. The monitoring for fault detection is performed by training a classifier that automatically orders or categorizes data into healthy and faulty cases by adapting machine learning algorithms. This is performed by feeding 70% of the healthy and faulty data into the

classifier for training and using the remaining 30% of the data for validating the trained classifier. The healthy case is defined as a case where no fault is present in any component within the system. To improve the sensitivity of the simulation model, the deviation identified between the healthy case of the simulated and the experimental data is utilized to augment the simulation data by adding the deviation to all simulation data. This deviation between the simulation and the experimental data arises due to environmental conditions, sensor uncertainties, and other components of the system. The deviation obtained from the healthy experimental data under a certain operating condition is added to the data generated from the simulation model creating augmented simulation data. This approach is different from the traditional approach of filtering noise from experimental data. The augmented simulation data can be used for real-time condition monitoring and require no data pre-processing as in the case of conventional condition monitoring methods.

In this paper, a simulation model of the hydraulic axial piston pump is developed in the MATLAB / Simulink environment. The model is validated by utilizing the available experimental dataset containing the healthy and the faulty cases; A classifier is trained to classify data into healthy, fault I, and fault II cases, respectively. The remainder of the paper is as follows. Section 2 provides information on the methodology and contains subsections on the simulation model, simulation parameters and data structure, and data analysis. In Section 3, data analysis is performed for healthy and faulty cases. Section 4 concludes the paper and provides insights for future development.

2 Methodology

In section 2.1, the simulation model developed in MATLAB/Simulink is explained in detail. In section 2.2, the parameters used in the simulation model and the data structure are described.

2.1 Pump Model

The three main friction pairs in axial piston pumps are the swash plate and the slipper [14], the valve plate and the cylinder block, and the piston and the cylinder bore [9], [15]. The most common failure in axial piston pumps is wear of these components. All three of these faults eventually lead to the failure of the pump. Usually, these types of faults are caused by contaminated fluid [16], but other factors such as varying load, can increase the wear rate [9], [15]. The wear between the valve plate and the cylinder block can be caused by the fluctuating load and unbalanced pressure distribution and it can be detected as increased leakages and vibrations [15]. Internal leakages in the pump lead to decreased volumetric efficiency.

The axial piston pump model utilized above presented information and was modelled using MATLAB/Simulink. Similar axial piston pump models have been previously used to study flow ripples [17] and leakages [18], [19].

The pressures in different sections of the pump are calculated using the continuity equation

$$\frac{dP}{dt} = -\frac{B}{V}(Q_{in} - Q_{out}), \tag{1}$$

where B is the bulk modulus, V is the instantaneous volume of the chamber, Q_{in} is the flow from into the chamber and Q_{out} is the output flow from the mentioned chamber, which contains the possible leakages. Equation (1) is used to calculate pressures in different piston chambers, in discharge chamber as well as the output pressure.

The flows in different sections of the pump are calculated using classical orifice equation

$$Q = sign(\Delta p) C_d A_v \sqrt{\frac{2\Delta p}{\rho}}, \tag{2}$$

where Δp is the pressure difference over the orifice, C_{d} is the discharge coefficient, A_{v} is the cross-section area of the orifice, and ρ is the fluid density. Equation (2) is used to calculate input flow from the tank to piston chambers through the valve plate, output flow from the piston chambers to discharge chamber through the valve plate and the output flow from the discharge chamber into the system.

In an axial piston pump, three main leakages can occur during operation. These leakages are modelled as following: piston, slipper and swash plate, and valve plate and cylinder block.

The leakage in a single piston can be described as [23]

$$Q_{lpn} = \frac{\pi\delta_p^3}{6\mu L}\Delta p, \tag{3}$$

where r is the radius of the piston, δ_p is the clearance between the piston and the cylinder block, μ is the kinematic viscosity, L is the length of leakage passage, and Δp in this equation is the pressure difference between the piston chamber and the case drain chamber.

The leakage between single slipper and the swash plate is represented using [23]

$$Q_{lsn} = \frac{\pi d_{lh}^4 \delta_s^3}{\mu(6d_{lh}^4 \ln\left(\frac{R_s}{r_s}\right)+128\delta_s^3 l_p}\Delta p, \tag{4}$$

where d_{lh} is the diameter of the piston leakage hole, δ_s is the clearance between the slipper and the swash plate, R_s and r_s are the outer and inner radii of the slipper respectively, and l_p is the length of the piston. The leakage occurring between valve plate and cylinder block can be modelled with [23]

$$Q_{lv} = \frac{d_v^3}{12\mu}\left(\frac{1}{\ln\left(\frac{R_2}{R_1}\right)} + \frac{1}{\ln\left(\frac{R_4}{R_3}\right)}\right)\Delta p, \tag{5}$$

where δ_v is the clearance between the valve plate and the cylinder block, R_1 and R_2 are the inside and outside radii of the inside valve plate seal ring respectively, R_3 and R_4 are the inside and outside radii of the outside valve plate seal ring. Regarding the leakage between the valve plate and the cylinder block, Δp is the pressure difference between the discharge port and the case drain chamber.

Figure 1 presents the main parts of the model, including 9 pistons, the leakage between the valve plate and the cylinder block, output pressure, flow, torque, and volumetric displacement.

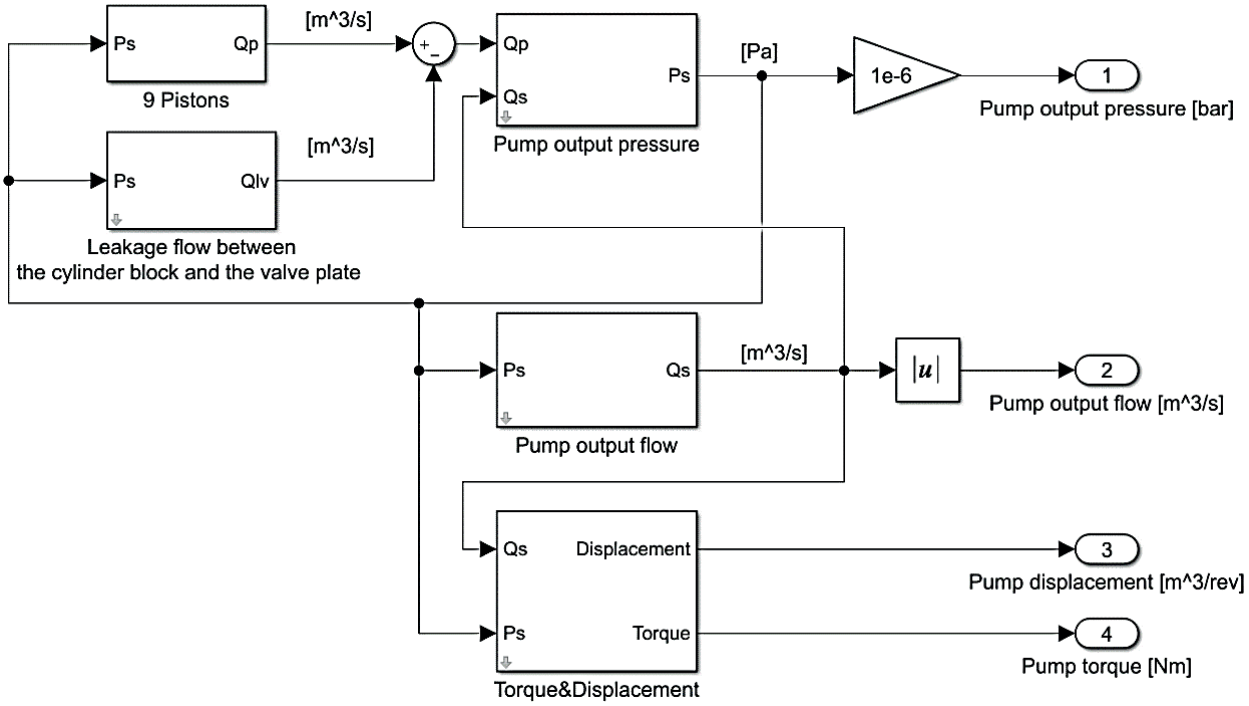

Figure 1: MATLAB/Simulink model of axial piston pump

Figure 2 contains the subparts which are used to model flow of a single piston. The subparts include the leakage between the piston and the cylinder block, the leakage between the slipper and the swash plate, stroke and velocity of the piston, the discharge areas of the piston port, input and output flow of the piston chamber, and the instantaneous pressure in the piston chamber.

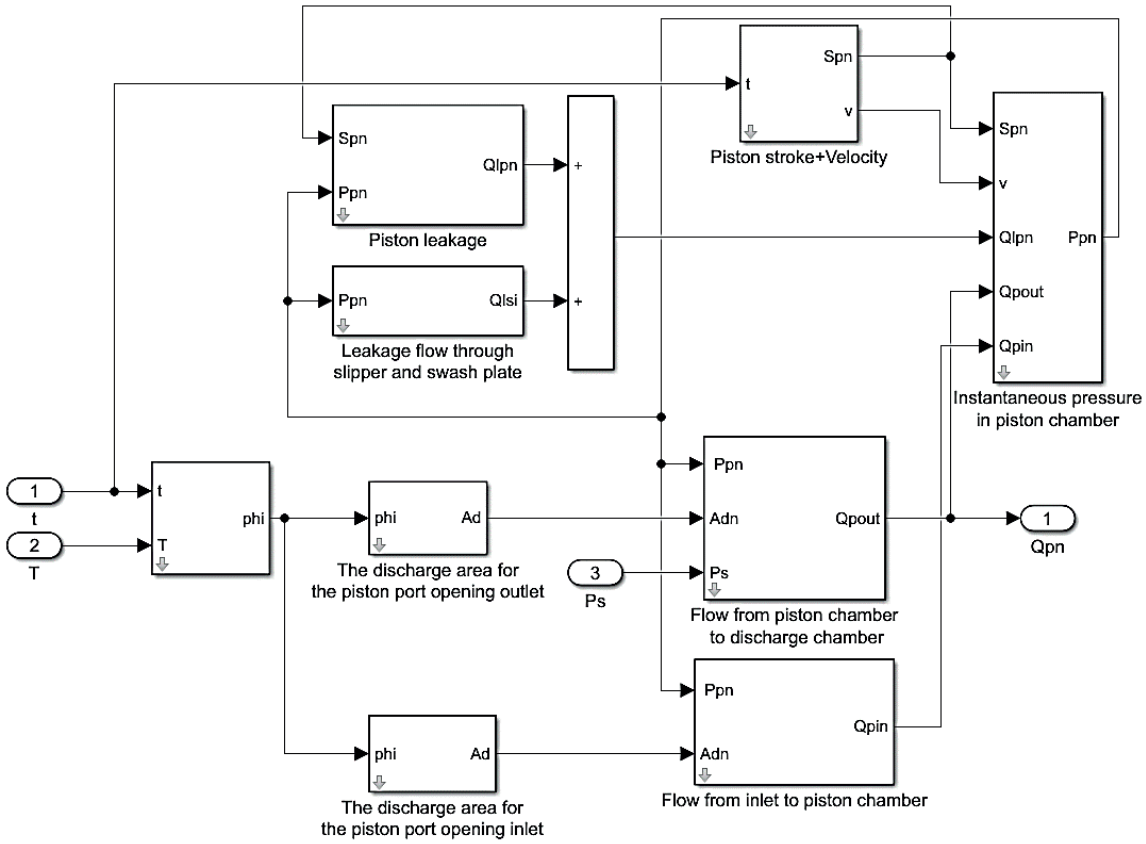

Figure 2: MATLAB/Simulink model of a piston

2.2 Simulation Parameters, Data Structure, and Test Rig

The selected pump model includes nine pistons, and it is assumed that the operation of the pump begins when one of the pistons is at the top dead center where the fluid begins to be compressed. The assumptions made regarding the model include the constant speed from the drive, the atmosphere tank pressure, the constant fluid density, and the temperature. Each simulation run is performed for a duration of 300 seconds, and the time step is 0.01s. The data points in each simulation run are 30,000 and 27 simulation runs are performed to generate data for all cases. The cases are generated by updating the load pressure parameter in the simulation model and the rotational speed parameter.

The data structure is presented in **Table 1.** The data is divided into healthy (H), fault I (F-I), and fault II (F-II) classes, respectively, and further subdivided into the cases. The healthy case is when no fault is present in the system. Fault I and Fault II are injected into the system by changing the parameters in the simulation model. The changed parameters include the clearance value between the valve plate and cylinder block for fault I and the clearance value between the slipper and swash plate for fault II.

For a clear understanding, experimental is abbreviated as EXP, simulation is abbreviated as SIM, and augmented simulation is abbreviated as AUG SIM throughout this paper. The parameters that are extracted (as training data) from the simulation model are pressure (bar), torque (Nm), flow (m^3/s), and volumetric displacement (m^3/rev). The parameters available in the experimental data (for validation purpose) include pressure and torque and are available in the same units.

Case	Pressure (bar)	Rotational Speed (RPM)	Healthy (H)	Fault I (F-I)	Fault II (F-II)
A	50	500	H_A	F-I_A	F-II_A
B	150	500	H_B	F-I_B	F-II_B
C	250	500	H_C	F-I_C	F-II_C
D	50	1500	H_D	F-I_D	F-II_D
E	150	1500	H_E	F-I_E	F-II_E
F	250	1500	H_F	F-I_F	F-II_F
G	50	2000	H_G	F-I_G	F-II_G
H	150	2000	H_H	F-I_H	F-II_H
I	250	2000	H_I	F-I_I	F-II_I

Table 1: Case Description

The schematic for the experimental test rig is illustrated in **Figure 3.** The experimental data is generated from the test rig by utilizing a piezo electric (quartz) sensor for measuring the pressure ripple. KISTLER 6005 is the model of the sensor and has a range of 0-1000 bar, natural frequency of 140 kHz, and 0.8% full scale accuracy. A flow meter with a range of 80 L/min is used to obtain the flow in the system. A torque meter with a range of 0-500 Nm and a maximum rotational speed of 12000 RPM is also utilized to measure the torque in the system.

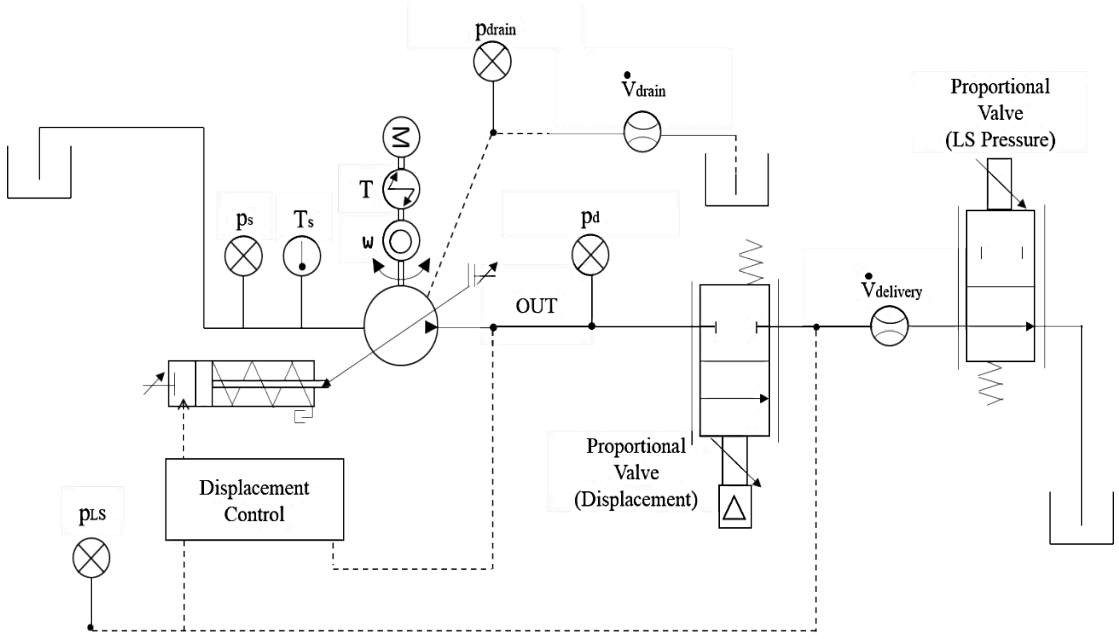

Figure 3: Experimental Test Rig Schematic

3 Data Analysis

The data analysis is performed to validate the simulation data with the experimental data. The raw signal is plotted to compare the simulated data with the experimental data in section 3.1. The validation is then performed by plotting the power spectrum density in section 3.2. Cases A, E, and I are selected as presented cases in this paper for clarity. Faulty cases E and I are also plotted for power spectrum density validation.

3.1 Data Analysis with healthy data using raw signals

Figure 4 represents the comparison plot for pressure data of healthy cases A, E, and I for experimental and simulation data on the left-side. The simulation data is quite close to the experimental data for cases A and E. In case I, a larger deviation can be noticed, however, the mean of the experimental signal and simulated signal are nearly the same. The experimental data carries noise while the simulation data is pure and ideal. The source of noise

produced in the experimental data could be due to the environmental conditions under which the experiment was conducted as well as from the utilized sensors. In simulation data, environmental effects are not considered and hence a cleaner set of data is produced. It could also mean that the simulation model has limitations and that it does not work at high RPM. To account for this deviation between experimental and simulation data, the simulation pressure signal for healthy case is subtracted from experimental pressure signal. This value of deviation is added to all the simulation run cases. The simulated data with the added deviation is referred to as augmented simulation data (AUG SIM). Also, figure 3 demonstrates the comparison plot for pressure data of healthy cases A, E, and I for experimental and simulation data on the right-side. The deviation added to all simulated signals are derived by subtracting the healthy simulation case A from experimental case. Hence, for case A, the experimental and augmented simulation signal overlap. For case E, higher peaks have formed for the augmented simulation signal while they were lower in the case of simulation signal. For case I, magnitude of pressure is closer to the experimental data behavior when compared to the simulated signal behavior.

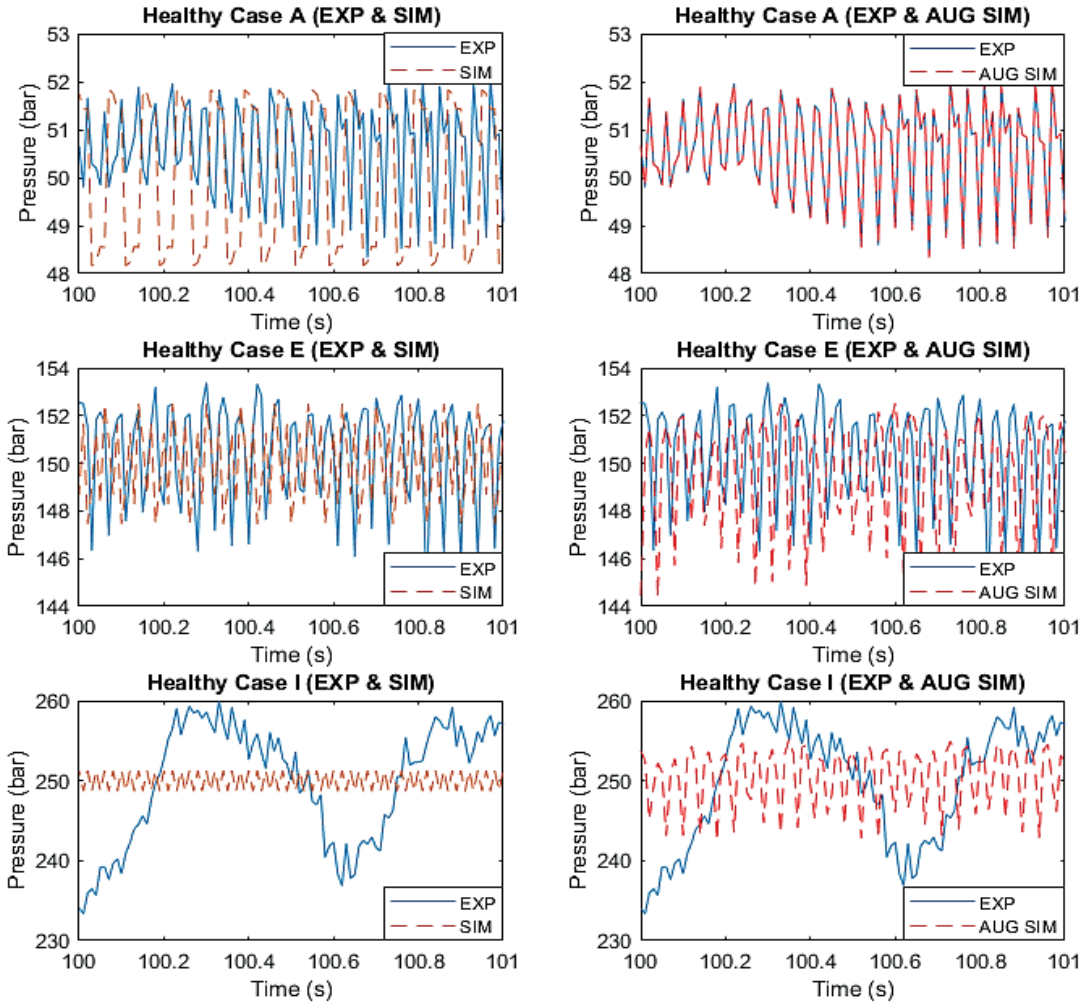

Figure 4: The left-side column shows the experimental and simulation data comparison for healthy cases A, E, and I. The right-side column shows the experimental and augmented simulation data comparison for healthy cases A, E, and I

3.2 Data Analysis with healthy and failure data using power spectrum density

Spectral analysis is performed for data analysis and it accounts for the signals in their frequency domain. Healthy cases A, E, and I are chosen for performing spectral analysis. **Figure 5** illustrates the power density spectrum for healthy pressure signals. It can be noticed that for all three cases, the power spectrum of augmented simulation data is closer to the experimental data when compared to pure simulation data. The simulation data is far from experimental data by around 5 times for every case. A sample power spectrum density plot of fault I and fault II are illustrated in **Figure 6.**

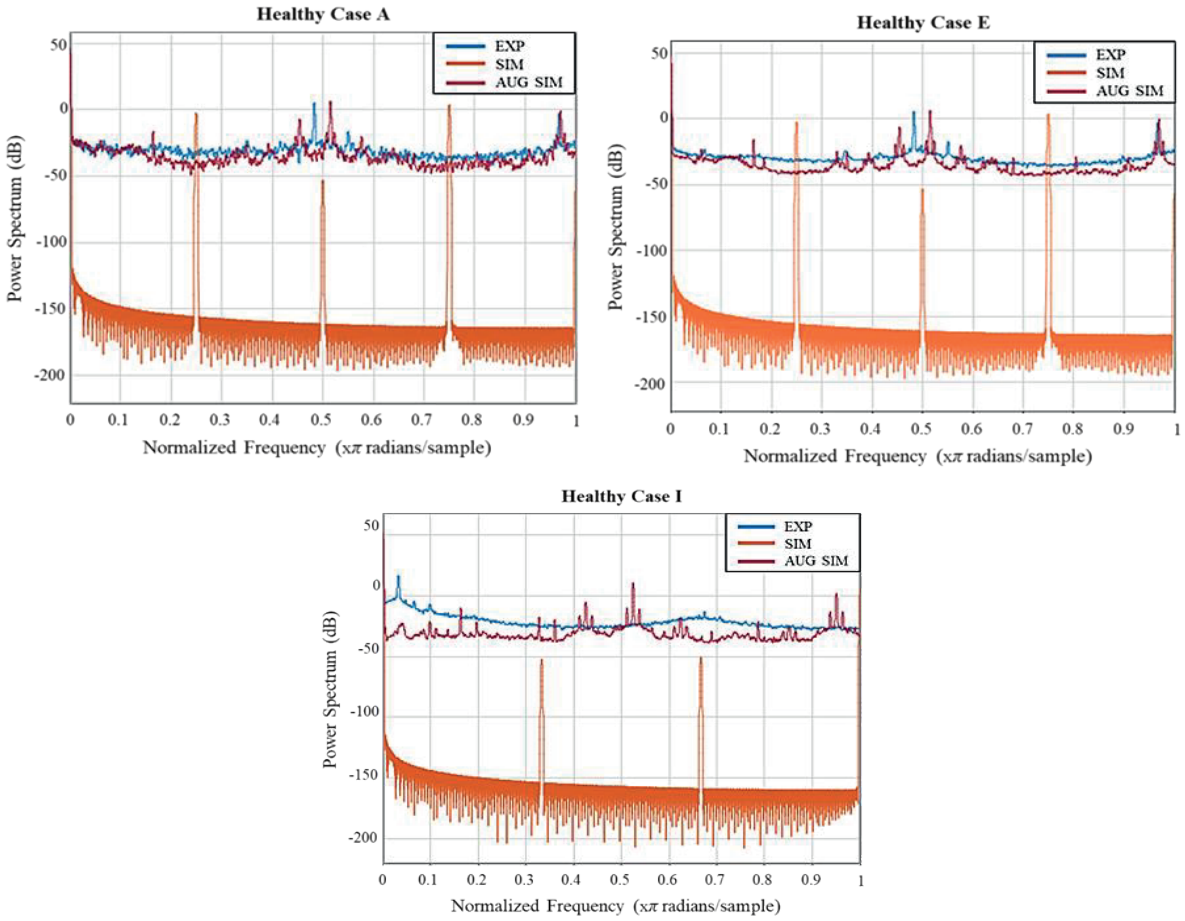

Figure 5: Sample power spectrum density plot for pressure data for selected healthy cases A, E, and I. Experimental is abbreviated as EXP, simulation is abbreviated as SIM, and augmented simulation is abbreviated as AUG SIM.

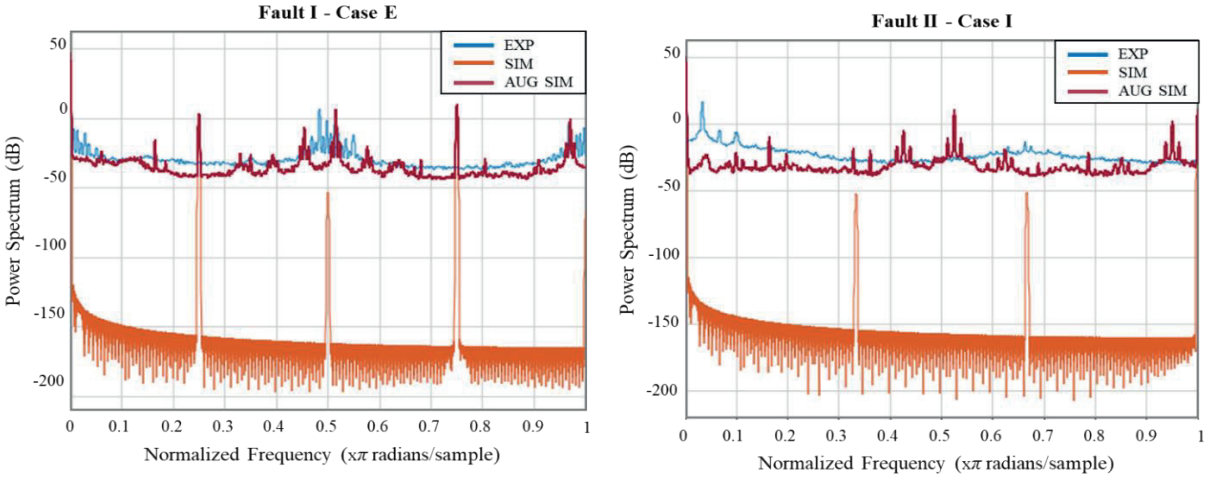

Figure 6: Sample power spectrum density plot for pressure data. The left side plot depicts Fault 1 pressure for case E. Right side plot depicts Fault II pressure for case I.

The augmented simulated signals (AUG) are closer to the experimental (EXP) power spectrum density when compared to the simulation data. This shows that the augmented simulation data is more reliable.

4 Results and Discussion

The main challenge of fault detection is data scarcity. Experimental data is often unavailable since the manufacturer of components do not always provide faulty component data and it is hard to inject real faults into components. The sensors may carry errors themselves which generate data that is not reliable. Also, the sensor calibration is critical as it also affect the quality of data obtained. Hence, it is important to develop a simulation model that can replace experiments. The data analysis section has shown that the data generated from the simulation model represent experimental data. To further check the performance of simulation model, classification is performed. Classification is used to distinguish between different faulty and healthy cases to identify the type of fault. This tool is used to diagnose the location of faults and reduce maintenance downtimes. A classifier trained by using machine learning algorithms. In this paper, three different classifiers for experimental simulation, and augmented simulation data are developed. Upon testing several machine learning algorithms [13], a multi-layer perceptron classifier turned out to be the best choice for the data at hand.

The various parameters that are used to analyze the classifiers are precision, recall, F1-score, and accuracy score. Precision is a machine learning tool that identifies the number of correct positive predictions made. Recall depicts the number of correct positive predictions made from all positive predictions that could have been made. F1-score is the weighted average of recall and precision. Accuracy score tells us how accurately the classifier can differentiate between all the fault types. The accuracy score is highest for experimental data followed by augmented simulation and simulation data.

The results obtained from the three classifiers are shown in **Table 2.** The classifier trained using the experimental data is capable of accurately distinguishing the fault type 88.7% of the time. The classifier trained using simulation and augmented simulation data are 70.1% and 75.7% accurate in distinguishing between the fault types. This implies that the augmented simulation data is suitable for on-line condition monitoring since it does not depend on additional signal processing techniques for denoising the signal.

Fault Type	Precision	Recall	F1-score	Accuracy Score	Data Type
Fault I (F-I)	0.86	0.82	0.84	**0.887**	Experimental
Fault II (F-II)	0.97	0.99	0.98		
Healthy (H)	0.83	0.85	0.84		
Fault I (F-I)	0.59	0.61	0.6	**0.701**	Simulation
Fault II (F-II)	0.84	1.00	0.91		
Healthy (H)	0.64	0.49	0.56		
Fault I (F-I)	0.72	0.44	0.55	**0.757**	Augmented Simulation
Fault II (F-II)	1	0.97	0.98		
Healthy (H)	0.61	0.86	0.71		

Table 2: MLP Classifier results for experimental, simulation without noise, and simulation with noise

To visualize the classifiers better, a confusion matrix is generated for experimental and augmented simulation data type as presented in **Figure 7**. It provides a visual representation of actual versus predicted cases. For the augmented simulation data, the classifier is inaccurate for fault types healthy and fault II. This implies that the two cases share similarity and, hence, has contributed to the lower accuracy score of 75.7%.

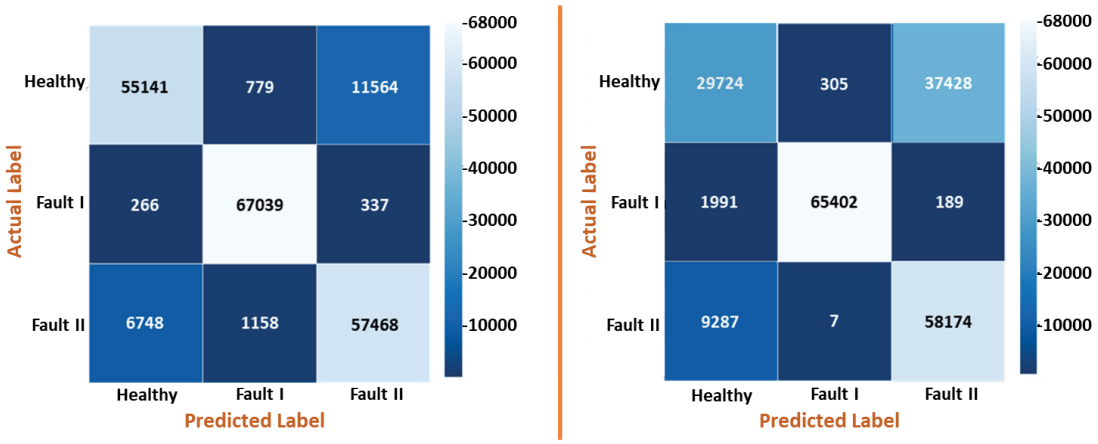

Figure 7: Confusion Matrices. Left side represents experimental data. Right side represents augmented simulation data

Training the classifier with additional data generated using the simulation model can bring further improvement and increase the accuracy. The accuracy obtained using the augmented simulation data can be further improved by generating additional data for the same cases. Generating too much data can also lead to challenges in classification. An overfit machine learning model refers to a model that has learned the details and noise in the training data to an extent that it negatively impacts the performance of the model on new data. The current accuracy scores are obtained by considering the same number of data points for each data type.

There are several reasons for the difference in accuracy scores between the data types. Firstly, the simulation model have certain limitations such as not considering or neglecting certain parameters that contribute to losses. (This will be investigated as a part of future study) Secondly, the crank angle of the piston might not be the same in the simulation and experimental cases. Lastly, certain experimental errors could also occur during performing measurements. (It is planned to repeat experiments in IHA laboratories as a part of future study).

5 Conclusion and Future developments

Overall condition monitoring and fault detection of hydraulic systems are instrumental to reduce the maintenance cost and to prevent the system from deteriorating by detecting the fault in its incipient stage. The condition monitoring system generally involves integration of additional sensors to the system under study for fault detection and diagnosis. However, such systems are themselves costly and are sensitive to faults. Consequently, the current trend is artificial intelligence (AI)-based condition monitoring . These methods rely on data generated from multi-sensor measurements rather than utilizing simulation models for condition monitoring as in the case of conventional condition monitoring.

In this paper, simulation model data is used as a source of training data for AI-based condition monitoring. To improve the sensitivity of the simulation model, the deviation identified between the healthy case of simulated and experimental data is used to augment the simulation data by adding the deviation to all simulation data. Data analysis is performed to validate the simulation data with available experimental data. The augmented simulation data turned out to be closer to the experimental data when compared to simulation data. To test the reliability of simulation data, an AI based classifier is developed that can distinguish faulty and healthy cases. The accuracy scores obtained for the three developed classifiers for experimental, simulation, and augmented simulation data are 88.7%, 70.1%, and 75.7%, respectively.. The added advantage of augmented simulation data is that pre-processing of online data will not be required as the augmented simulation data carries information about the noise that are present in experimental conditions. Hence, the augmented simulation data is a suitable candidate for online condition monitoring.

For future development, additional data can be generated for various faults and fed to AI-based classifiers for fault detection and to reduce maintenance breakdown times. Validation with experimental data that contains other parameters such as flow and displacement can be used to further improve the performance of the simulation model. The end goal is to develop a software and data acquisition system that is capable of condition monitoring of axial piston pump by utilizing the trained classifier.

6 Acknowledgements

This work was enabled by the financial support of Academy of Finland (project ESTV) and internal funding from the Department of Automation Technology and Mechanical Engineering, IHA group at Tampere University, Finland.

Nomenclature

Variable	Description	Unit
A_v	Discharge orifice area	[m^2]
B	Bulk modulus	[Pa]
C_d	Discharge coefficient	[-]
d_{lb}	Diameter of the piston leakage hole	[m]
L	Length of leakage passage	[m]
l_p	Length of the piston	[m]
$\triangle p$	Pressure difference	[Pa]
R_1	Inside radius of the inside valve plate seal ring	[m]
R_2	Outside radius of the inside valve plate seal ring	[m]
R_3	Inside radius of the outside valve plate seal ring	[m]
R_4	Outside radius of the outside valve plate seal ring	[m]
r	Radius of the piston	[m]
R_s	Outer radius of the slipper	[m]
r_s	Inner radius of the slipper	[m]
δ_p	Clearance between the piston and the cylinder block	[m]
δ_s	Clearance between the slipper and the swash plate	[m]
δ_v	Clearance between the valve plate and the cylinder block	[m]
μ	Kinematic viscosity	[m^2/s]
ρ	Fluid density	[kg/m^3]

References

[1] H. Tang, W. Yang, and Z. Wang, "*A Model-Based Method for Leakage Detection of Piston Pump under Variable Load Condition*," IEEE Access, vol. 7, pp. 99771–99781, 2019, doi: 10.1109/ACCESS.2019.2930816.

[2] J. Dai, J. Tang, S. Huang, and Y. Wang, "*Signal-Based Intelligent Hydraulic Fault Diagnosis Methods: Review and Prospects*," Chinese J. Mech. Eng. (English Ed., vol. 32, no. 1, 2019, doi: 10.1186/s10033- 019-0388-9.

[3] P. Casoli, M. Pastori, F. Scolari, and M. Rundo, "*A vibration signal-based method for fault identification and classification in hydraulic axial piston pumps*," Energies, vol. 12, no. 5, 2019, doi: 10.3390/en12050953.

[4] A. A. Azeez, M. Alkhedher, M. S. Gadala, and O. A. Mohamad, "*Fault Detection of Rolling Element Bearings using Advanced Signal Processing Technique*," in 2020 Advances in Science and Engineering Technology International Conferences (ASET), 2020, pp. 1–6, doi: 10.1109/ASET48392.2020.9118398.

[5] P. Casoli, A. Bedotti, F. Campanini, and M. Pastori, "*A methodology based on cyclostationary analysis for fault detection of hydraulic axial piston pumps*," Energies, vol. 11, no. 7, 2018, doi: 10.3390/en11071874.

[6] P. Casoli, M. Pastori, and F. Scolari, "*A multi-fault diagnostic method based on acceleration signal for a hydraulic axial piston pump*," AIP Conf. Proc., vol. 2191, no. December 2019, doi: 10.1063/1.5138770.

[7] P. Casoli, F. Campanini, A. Bedotti, M. Pastori, and A. Lettini, "*Overall Efficiency Evaluation of a Hydraulic Pump with External Drainage Through Temperature Measurements*," J. Dyn. Syst. Meas. Control. Trans. ASME, vol. 140, no. 8, pp. 1–9, 2018, doi: 10.1115/1.4039084.

[8] A. A. Azeez, M. Alkhedher, and M. S. Gadala, "*Thermal Imaging Fault Detection for Rolling Element Bearings*," in 2020 Advances in Science and Engineering Technology International Conferences (ASET), Feb.

2020, pp. 1–5, doi: 10.1109/ASET48392.2020.9118361.

[9] Y. Lan et al., "*Fault diagnosis on slipper abrasion of axial piston pump based on Extreme Learning Machine*," Meas. J. Int. Meas. Confed., vol. 124, no. March, pp. 378–385, 2018, doi: 10.1016/j.measurement.2018.03.050.

[10] L. Yafei, J. Wanlu, N. Hongjie, S. Xiaodong, and Y. Xukang, "*Fault Diagnosis of Axial Piston Pump Based on Extreme-Point Symmetric Mode Decomposition and Random Forests*," Shock Vib., vol. 2021, 2021, doi: 10.1155/2021/6649603.

[11] W. L. Jiang, P. Y. Zhang, M. Li, and S. Q. Zhang, "*Axial Piston Pump Fault Diagnosis Method Based on Symmetrical Polar Coordinate Image and Fuzzy C-Means Clustering Algorithm*," Shock Vib., vol. 2021, 2021, doi: 10.1155/2021/6681751.

[12] S. Tang, S. Yuan, Y. Zhu, and G. Li, "*An integrated deep learning method towards fault diagnosis of hydraulic axial piston pump*," Sensors (Switzerland), vol. 20, no. 22, pp. 1–20, 2020, doi: 10.3390/s20226576.

[13] A. A. Azeez, X. Han, V. Zakharov, & T. Minav. "*AI-Based Condition Monitoring of Hydraulic Valves in Zonal Hydraulics Using Simulated Electric Motor Signals*." Proceedings of the ASME/BATH 2021 Symposium on Fluid Power and Motion Control. ASME/BATH 2021 Symposium on Fluid Power and Motion Control. Virtual, Online. October 19–21, 2021. V001T01A016. ASME. doi: 10.1115/FPMC2021-68615.

[14] J. Ma, J. Chen, J. Li, Q. Li, and C. Ren, "*Wear analysis of swash plate/slipper pair of axis piston hydraulic pump*," Tribol. Int., vol. 90, pp. 467–472, 2015, doi: 10.1016/j.triboint.2015.05.010.

[15] J. Du, S. Wang, and H. Zhang, "*Layered clustering multi-fault diagnosis for hydraulic piston pump*,"

Mech. Syst. Signal Process., vol. 36, no. 2, pp. 487–504, 2013, doi: 10.1016/j.ymssp.2012.10.020.

[16] X. Wang, S. Lin, S. Wang, Z. He, and C. Zhang, "*Remaining useful life prediction based on the Wiener process for an aviation axial piston pump*," Chinese J. Aeronaut., vol. 29, no. 3, pp. 779–788, 2016, doi: 10.1016/j.cja.2015.12.020.

[17] C. Guan, Z. Jiao, and S. He, "*Theoretical study of flow ripple for an aviation axial-piston pump with damping holes in the valve plate*," Chinese J. Aeronaut., vol. 27, no. 1, pp. 169–181, 2014, doi: 10.1016/j.cja.2013.07.044.

[18] B. Zhang, J. Ma, H. Hong, H. Yang, and Y. Fang, "*Analysis of the flow dynamics characteristics of an axial piston pump based on the computational fluid dynamics method*," Eng. Appl. Comput. Fluid Mech., vol. 11, no. 1, pp. 86–95, 2017, doi: 10.1080/19942060.2015.1091686.

[19] J. M. Bergada, S. Kumar, D. L. Davies, and J. Watton, "*A complete analysis of axial piston pump leakage and output flow ripples*," Appl. Math. Model., vol. 36, no. 4, pp. 1731–1751, 2012, doi: 10.1016/j.apm.2011.09.016.

[20] H. Deng, Q. Wang, P. Dai, and Y. Yang, "*Study on Leaking Characteristics of Port Plate Pair in Primary Three-Row Axial Piston Pump/Motor*," Math. Probl. Eng., vol. 2018, 2018, doi: 10.1155/2018/7395727.

[21] C. Bayer and O. Enge-Rosenblatt, "*Modeling of hydraulic axial piston pumps including specific signs of wear and tear*," Proc. from 8th Int. Model. Conf. Tech. Univeristy, Dresden, Ger., vol. 63, pp. 461–466, 2011, doi: 10.3384/ecp11063461.

[22] A. Roccatello, S. Mancó, and N. Nervegna, "*Modelling a variable displacement axial piston pump in a multibody simulation environment*," J. Dyn. Syst. Meas. Control. Trans. ASME, vol. 129, no. 4, pp. 456– 468, 2007, doi: 10.1115/1.2745851.

[23] J. Ivantysyn and M. Ivantysynova, "*Hydrostatic pumps and motors: principles, design, performance, modelling, analysis, control and testing*", Tech Books International, 2003, ISBN: 8188305081 9788188305087